IEEE Access
Multidisciplinary ⋮ Rapid Review ⋮ Open Access Journal

Received 12 July 2024, accepted 31 July 2024, date of publication 5 August 2024, date of current version 13 August 2024.

Digital Object Identifier 10.1109/ACCESS.2024.3438122

RESEARCH ARTICLE

Interclass Balance Factor-Based Membership Fusion Semi-Supervised Fuzzy Clustering Algorithm for Lesion Segmentation in Cerebral Infarction Images

BENFEI ZHANG[1,2], YIZHANG JIANG[1], (Senior Member, IEEE), AND KAIJIAN XIA[2,3]
[1]School of Artificial Intelligence and Computer Science, Jiangnan University, Wuxi, Jiangsu 214122, China
[2]Changshu Key Laboratory of Medical Artificial Intelligence and Big Data, Suzhou, Jiangsu 215500, China
[3]Center of Intelligent Medical Technology Research, Changshu Hospital Affiliated of Soochow University, Suzhou, Jiangsu 215500, China

Corresponding author: Kaijian Xia (kjxia@suda.edu.cn)

This work was supported in part by Jiangsu Province "333 Project" High-Level Talent Cultivation Subsidized Project, in part by Changshu Science and Technology Program under Grant CS202015 and Grant CS202246, in part by Changshu Key Laboratory of Medical Artificial Intelligence and Big Data under Grant CYZ202301 and Grant CS202314, and in part by Suzhou Key Supporting Subjects-Health Informatics under Grant SZFCXK202147.

ABSTRACT This study addresses the challenge of improving the accuracy and efficiency of lesion segmentation in brain stroke Diffusion Weighted Images (DWI), with a particular focus on the issue of class imbalance. Traditional clustering algorithms often fail to effectively segment brain stroke lesions due to the significantly smaller area of lesion regions compared to other brain tissues and background areas. To overcome this, we propose an Interclass Balance Factor-based Membership Fusion Semi-supervised Fuzzy Clustering Algorithm (ICBF-MFSFCM). This novel algorithm introduces an interclass balance factor to enhance the precision and consistency of clustering outcomes by better representing minority classes. The method was validated on actual brain DWI image datasets, demonstrating its superiority and reliability in improving lesion segmentation accuracy. The experimental results show that ICBF-MFSFCM outperforms traditional clustering algorithms in terms of Dice Coefficient (DSC), Intersection over Union (IoU), F1-score, and Surface Dice Similarity Coefficient (SDSC). These improvements offer a more efficient approach for the preliminary detection and treatment of cerebral stroke, contributing to better clinical outcomes for patients.

INDEX TERMS Medical image segmentation, interclass balance, semi-supervised clustering, interclass balance factor, membership fusion mechanism.

I. INTRODUCTION

High-quality medical image segmentation plays a pivotal role in identifying and managing brain stroke. It can enhance the accuracy of diagnoses, especially through automated segmentation methods such as decision tree classifiers and deep learning models. These technologies aid in more accurately determining lesion areas, facilitating early detection and effective treatment of brain stroke [1]. Moreover, accurate image segmentation helps physicians better understand the nature and extent of lesions, enabling them to develop more effective treatment plans and expedite the decision-making process, especially in cases of acute stroke [2].

However, medical image segmentation faces challenges and limitations in processing Diffusion Weighted Images (DWI) and segmenting brain stroke lesions. For example, the quality of DWI images and the diversity of lesions can impact segmentation accuracy. The complexity of lesion shapes, sizes, and boundaries are major difficulties [3]. Furthermore, although existing segmentation methods, such as

The associate editor coordinating the review of this manuscript and approving it for publication was Kumaradevan Punithakumar.

deep learning models, are effective, their design and training processes can be quite complex, requiring extensive data and computational resources. Moreover, for complex cases, these automated methods still necessitate the knowledge and experience of professional physicians to interpret and validate segmentation results [4], [5], [6], [7], [8]. Overall, despite the critical role of high-quality medical image segmentation in diagnosing and treating brain stroke, it still faces challenges regarding image quality, algorithm complexity, and dependence on professional expertise. Therefore, continuous technological innovation and the integration of professional knowledge are key to optimizing this field [9], [10], [11], [12], [13].

Semi-supervised fuzzy clustering algorithms have shown significant potential in the field of medical image segmentation, especially in handling complex images with uncertainties and noise. The key advantage of this approach lies in its combination of the flexibility of fuzzy clustering with the data efficiency of semi-supervised learning. For instance, the seed-based FCM algorithm proposed by Santos et al. utilizes information provided by doctors as constraints to enhance the determinacy of grouping, effectively improving the detection and segmentation of regions of interest in medical images [14]. Miao et al. developed an improved FCM algorithm that incorporates adaptive dictionary learning to reduce noise and enhance segmentation precision [15]. Moreover, the research by Chen et al. achieved efficient semi-supervised segmentation by combining unsupervised and semi-supervised learning strategies, using deep learning neural networks [16]. Semi-supervised fuzzy clustering methods can also overcome some limitations of traditional methods, such as improving robustness to noise and image heterogeneity. The application of this method in medical image segmentation, as demonstrated by Dubey et al., can effectively handle the uncertainties and fuzziness in MR brain images while maintaining high accuracy [17]. Tuan et al. research further extended this approach by using dynamic semi-supervised clustering, utilizing different predefined membership matrices to adapt to the unique structures of each image [18]. Studies by Le Son et al. and Kumar et al. have shown that this method enhances the efficiency and accuracy of segmentation, reducing dependence on extensive annotated data [19], [20].

Overall, semi-supervised fuzzy clustering methods, by integrating various techniques and strategies, bring new possibilities to the field of medical image segmentation. This approach not only improves the precision and robustness of segmentation but also reduces reliance on annotated data, making it an effective tool for handling complex medical images. These studies indicate that semi-supervised fuzzy clustering will play an increasingly significant role in future medical image processing, especially in situations of data scarcity and poor image quality.

The aim of this study is to enhance the precision and efficiency of brain stroke DWI image segmentation by proposing and evaluating a suitable semi-supervised fuzzy clustering approach. We expect this method to better handle the issue of class imbalance in images, providing more accurate lesion identification and, thus, more reliable information for the diagnosis and treatment of brain stroke. Through this research, we hope to offer a more effective tool for the early diagnosis and treatment of brain stroke, ultimately improving clinical outcomes for patients.

In segmenting brain stroke DWI images, we have found that traditional semi-supervised clustering often performs poorly in brain stroke lesion segmentation tasks [21], [22], [23], [24]. The reason lies in the significantly smaller area of brain stroke lesion regions compared to other brain tissue and background areas at many times, leading to severe class imbalance issues in clustering. In the field of distance-based clustering, addressing class imbalance remains a complex challenge. Traditional clustering methods such as K-means, Fuzzy C-means and hierarchical clustering often fail to represent minority classes accurately due to their relatively smaller size. This results in a skewed clustering process that tends to favor larger classes, thereby overlooking the distinct characteristics of smaller groups. Various strategies have been developed to tackle this imbalance, as shown Table 1, in each with its own set of advantages and limitations.

TABLE 1. The comparison table for methods dealing with class imbalance in distance-based clustering.

Method	Representative Algorithms	Advantages	Disadvantages
Resampling	SMOTE for Clustering[25]	Directly adjusts data distribution, enhances minority influence	May lead to overfitting or information loss
Modifying Distance Metrics	Weighted K-Means[26]	Adjusts focus through weights, improves recognition of small classes	Proper weight selection needed, may increase computational complexity
Ensemble Methods	Cluster Ensembles[27]	Improves stability and accuracy, captures data structure from multiple angles	High computational cost, dependent on the quality of individual clustering results
Density-Based Methods	DBSCAN[28], OPTICS[29]	No need to specify cluster numbers, naturally handles different densities, effectively identifies noise and outliers	Sensitive to parameters, performance may decline with high-dimensional data
Using Prior Knowledge	SFCM[30], Constrained K-Means[31]	Utilizes prior knowledge to enhance clustering accuracy and interpretability, prevents incorrect clustering	Requires prior knowledge, constraints may limit algorithm flexibility

Resampling techniques, such as the Synthetic Minority Over-sampling Technique (SMOTE) [25], adjust the class distribution by oversampling minority classes or undersampling majority classes. While effective in balancing the dataset and enhancing the fairness of the clustering process, these techniques can lead to overfitting or significant data

loss, depending on whether oversampling or undersampling is used.

Another approach is modifying distance metrics within algorithms like Weighted K-Means [26], where data points are assigned weights based on their class size to amplify the influence of minority classes during the clustering process. This method integrates smoothly into existing algorithms and improves the representation of smaller classes. However, it requires careful calibration of weights, which can complicate the clustering process and increase computational overhead.

Ensemble methods, such as Cluster Ensembles [27], combine multiple clustering outputs to achieve a more stable and accurate outcome. These methods are beneficial as they capture multiple facets of the data structure, offering a comprehensive view that mitigates biases inherent in single-run models. Despite their robustness, they are computationally intensive and their effectiveness largely depends on the quality of individual clustering results.

Density-based methods like Density-Based Spatial Clustering of Applications with Noise (DBSCAN) [28] and Ordering Points To Identify the Clustering Structure (OPTICS) [29] excel in handling clusters of varying densities and are less affected by class sizes. These methods are particularly adept at identifying outliers and noise, crucial for datasets with diverse class distributions. However, their effectiveness is contingent on precise parameter settings and they often struggle with high-dimensional data.

The Constrained K-Means algorithm [31], which incorporates prior knowledge through constraints like must-link or cannot-link, enhances clustering accuracy and interpretability. It ensures the clustering adheres to known relationships within the data. Nevertheless, this method depends on the availability of prior knowledge and may lack flexibility due to its constraints. The Semi-supervised Fuzzy C-means (SFCM) algorithm, which also utilizes prior knowledge, has similar drawbacks [30].

Inspired by methods that modify distance metrics and those using prior knowledge, this paper proposes an Inter-Class Balance Factor Membership Fusion Semi-Supervised Fuzzy Clustering Algorithm (ICBF-MFSFCM). On one hand, this study introduces an inter-class balance factor, where weights can be adjusted based on the distribution of categories within the dataset, thereby modifying the clustering distance metric. Through this approach, the algorithm can amplify the influence of smaller categories to accommodate various data distributions. In clustering algorithms, minority classes are often overshadowed by majority classes. By incorporating an inter-class balance factor, the algorithm more effectively captures the characteristics of these minority classes, thus enhancing the overall segmentation capability of the algorithm. On the other hand, the proposed algorithm employs a semi-supervised framework similar to the Semi-supervised Fuzzy C-Means (SFCM) [30] algorithm, integrating prior knowledge from labeled data to improve the accuracy and interpretability of clustering. Furthermore, this framework includes a membership fusion mechanism introduced by Zhang et al. [32] to ensure stable guidance of prior knowledge in clustering. These methods enhance the fairness of the algorithm towards all categories, ensuring that the algorithm does not favor larger categories but considers all categories equally.

Contributions of this paper: This paper presents an Inter-Class Balance Factor Membership Fusion Semi-Supervised Fuzzy Clustering Algorithm (ICBF-MFSFCM) that effectively addresses the issue of category imbalance. Compared to other distance-based clustering algorithms, it achieves superior and more stable performance in the task of cerebral infarction lesion segmentation in brain images. The effectiveness of the proposed ICBF-MFSFCM algorithm is validated through experiments conducted on a real-world brain image dataset.

II. RELATED WORK

A. FUZZY C-MEANS

The Fuzzy C-Means (FCM) algorithm is a clustering method proposed by J.C. Dunn in 1973 and further developed by J.C. Bezdek in 1981. It is an extension of the traditional k-means algorithm, designed to allow one piece of data to belong to two or more clusters. This method is particularly useful in the fields of pattern recognition and machine learning for handling datasets with overlapping or unclear boundaries between clusters [33].

The FCM algorithm classifies data by assigning membership levels between 0 and 1 to each data point for each cluster, indicating the degree to which each data point belongs to each cluster. Unlike k-means, where data strictly belong to one cluster, in FCM, data points can belong to multiple clusters with varying degrees of membership, reflecting the fuzzy nature of the classification.

The objective function of FCM is defined as:

$$J_m = \sum_{i=1}^{N} \sum_{j=1}^{C} u_{ij}^m |x_i - c_j|^2 \tag{1}$$

where N is the number of data points, C is the number of clusters, x_i is the ith data point, c_j is the center of the ith cluster, u_{ij} is the membership degree of x_i in the cluster j, m is the fuzziness index ($m > 1$), and $|x_i - c_j|$ is the Euclidean distance between x_i and c_j.

The FCM algorithm follows an iterative optimization process to minimize the objective function J_m, which balances the distance of data points from the cluster centers with the degree of their membership in the clusters. The steps are as follows:

(1) Initialization: Choose the number of clusters C and initialize the cluster centers randomly.
(2) Membership Update: For each data point and each cluster center, update the membership u_{ij} using the formula:

$$u_{ij} = \frac{1}{\sum_{k=1}^{C} \left(\frac{|x_i - c_j|}{|x_i - c_k|} \right)^{\frac{2}{m-1}}} \tag{2}$$

(3) Cluster Centers Update: Update the cluster centers c_j for each cluster using the formula:

$$c_j = \frac{\sum_{i=1}^{N} u_{ij}^m x_i}{\sum_{i=1}^{N} u_{ij}^m} \tag{3}$$

(4) Repeat: Repeat steps 2 and 3 until the changes in u_{ij} or c_j between two consecutive iterations are below a certain threshold, indicating that the algorithm has converged.

The choice of the fuzziness index m influences the level of cluster fuzziness; larger values result in fuzzier clusters. The FCM algorithm is widely used for its flexibility and effectiveness in producing soft clustering results, making it applicable to a variety of complex real-world problems.

B. SEMI-SUPERVISED FUZZY C-MEANS

The Semi-supervised Fuzzy C-Means (SFCM) algorithm, an advanced version of the traditional Fuzzy C-Means approach, integrates a portion of labeled data into the clustering mechanism. This method, pioneered by Pedrycz, seeks to improve clustering outcomes by leveraging both labeled and unlabeled data, offering a more nuanced analysis of data groupings [30].SFCM stands out by utilizing labeled data to influence the clustering of unlabeled data, thereby enhancing the algorithm's ability to discern the true structure of the dataset. This approach merges the exploratory nature of unsupervised learning with the directional guidance of supervised learning, aiming for more accurate and meaningful clusters.

The objective function of SFCM aims to balance the traditional fuzzy clustering criteria with a correction term that accounts for the discrepancy between the computed memberships and the true labels of the labeled data. The revised objective function is given by:

$$J_s = \sum_{i=1}^{c}\sum_{j=1}^{n} u_{ij}^m d_{ij}^2 + \alpha \sum_{i=1}^{c}\sum_{j=1}^{n} \left(u_{ij} - f_{ij} b_j\right)^m d_{ij}^2 \tag{4}$$

In this formula: c indicates the number of clusters, n the total number of points in the dataset, u_{ij} the membership degree of the jth data point to the ith cluster, d_{ij} the distance between the jth data point and the centroid of the ith cluster, m represents the fuzziness index, α is a parameter balancing supervised and unsupervised contributions, f_{ij} denotes the true membership of labeled data, b_j is a binary flag indicating whether a data point is labeled.

Optimizing the SFCM involves a cyclic process aimed at minimizing the objective function J_s through the following steps:

(1) Membership Adjustment: The algorithm recalculates the membership degrees u_{ij} for each data point by considering both their distance to cluster centroids and the labels of the labeled data.

(2) Centroid Recalculation: It updates the cluster centroids based on these new membership degrees, ensuring that each cluster center is pulled towards the points most strongly associated with it, while also respecting the influence of labeled samples.

This iterative process repeats until the adjustments to the objective function across iterations become negligible, signifying that the algorithm has stabilized and found an optimal clustering configuration. SFCM's strategy of incorporating labeled data into fuzzy clustering presents a sophisticated technique for improving cluster analysis. By melding the insights from labeled examples with the broader dataset, it achieves a more informed and accurate partitioning of the data, demonstrating the power of combining supervised insights with unsupervised learning methods.

III. INTERCLASS BALANCE FACTOR BASED MEMBERSHIP FUSION SEMI-SUPERVISED FUZZY C-MEANS

Within this part of the text, we propose an innovative objective function for fuzzy clustering incorporating an interclass balance factor relying on a mechanism for fusing memberships and derive an algorithm to minimize this objective function.

$$\begin{aligned} J = (1-\eta)\sum_{i=1}^{C}\sigma_i \sum_{j=1}^{N} u_{ij}^m d_{ij}^2 \\ + \eta\alpha \sum_{i=1}^{C}\sum_{j=1}^{N} b_j \left(\left|u_{ij} - f_{ij}\right|^m + u_{ij}^m\right) d_{ij}^2 \end{aligned} \tag{5}$$

This function (5) consists of two main parts:

(1) Unlabeled data loss: $(1-\eta)\sum_{i=1}^{C}\sigma_i \sum_{j=1}^{N} u_{ij}^m d_{ij}^2$, involving unlabeled data, where σ_i is the interclass balance factor, and m is the fuzzifier.

(2) Labeled data loss: $\eta\alpha \sum_{i=1}^{C} \sum_{j=1}^{N} b_j \left(\left|u_{ij} - f_{ij}\right|^m + u_{ij}^m\right) d_{ij}^2$, involving labeled data, where η is the supervision rate, α is an adaptive parameter, b_j is a Boolean value representing whether there is a label at j, f_{ij} is the supervisory information, such as the real label of the jth pixel on class i or the given known membership degree, and $\left(\left|u_{ij} - f_{ij}\right|^m + u_{ij}^m\right)$ is a membership fusion term, adopting the membership fusion mechanism proposed by Zhang in 2023 [32], aimed at achieving more stable clustering effects through the more stable influence of labeled data. The presence of u_{ij}^m in the supervisory term keeps it consistent with the unsupervised term, making it more intuitive and computationally convenient, where m serves the same function as in the standard FCM formula.

In the pursuit of achieving balance among different categories in unlabeled data, this study introduces an inter-class balance factor, $\boldsymbol{\sigma}$. This innovative measure aims to intuitively manage the varying degrees of influence each category has on the processing of unlabeled data. By adjusting the contributions of different categories, $\boldsymbol{\sigma}$ is designed to coordinate their impact, ensuring that no single category disproportionately affects the model's learning process from unlabeled data. Traditional fuzzy clustering algorithms encounter an

issue when the desired segmentation results involve large differences in category sizes: smaller categories, due to their fewer numbers, can tolerate higher values of $u_{ij}^m d_{ij}^2$, meaning the objective function does not sufficiently constrain their membership degrees. This often leads to the misclustering of members of smaller categories. Due to the characteristics of its objective function, traditional fuzzy clustering tends to cluster data into categories of similar sizes. Therefore, these smaller categories end up being classified into larger, semantically meaningless categories where they do not belong. This can be acceptable when the goal of clustering is to uncover hidden commonalities or patterns among data, but when clustering serves as a means for medical image segmentation, where the characteristics of the categories are known and the goal is to segment based on these features, the emergence of large but semantically void categories is undesirable and should be avoided. In traditional unsupervised clustering, it is difficult to directly introduce a factor to regulate category balance, as the order of the categories during the clustering process is random and unknown. Conversely, as this algorithm incorporates prior knowledge through $\left|u_{ij} - f_{ij}\right|^m$, the order of categories is no longer random but known before clustering, thus the resulting category semantics often align with expectations. Therefore, introducing the inter-class balance factor $\boldsymbol{\sigma}$ becomes a viable solution. Furthermore, this paper discusses the scenario of overall data category imbalance, assuming that the supervisory information between categories is balanced. This assumption is plausible because, unlike the overall data with category imbalance, balanced supervisory information is not difficult to obtain in clinical applications of image segmentation. Therefore, $\boldsymbol{\sigma}$ is introduced only in the unsupervised term to address the category imbalance in the overall data, resulting in $(1-\eta)\sum_{i=1}^{C}\sigma_i\sum_{j=1}^{N}u_{ij}^m d_{ij}^2$, without the need to introduce it into the supervision term corresponding to the labeled information.

Figure 1 and Figure 2 illustrate the effect of $\boldsymbol{\sigma}$ when $m = 2$. In these figures, when either $\boldsymbol{\sigma}$, membership, or distance is small, the individual unsupervised item is smaller; when membership or distance is 0, the individual unsupervised item

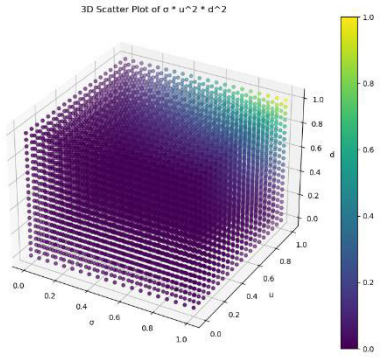

FIGURE 1. The value of $\sigma_i u_{ij}^2 d_{ij}^2$ and its relationship with the quantity of variables in a three-dimensional scatter plot.

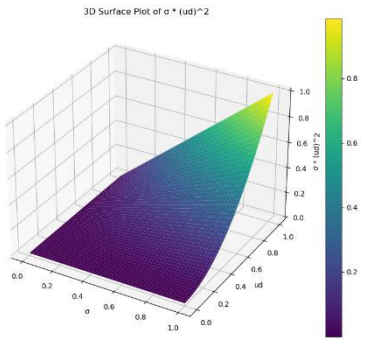

FIGURE 2. The influence of σ and ud on the value of $\sigma_i u_{ij}^2 d_{ij}^2$.

is minimized; and when all three values are large, it is larger. Therefore, when it is necessary for smaller categories not to be ignored, setting a larger $\boldsymbol{\sigma}$ for that category makes the objective function more sensitive to $u_{ij}^m d_{ij}^2$ for that category, encouraging smaller $u_{ij}^m d_{ij}^2$ values, and vice versa. The introduction of the interclass balance factor $\boldsymbol{\sigma}$ aims to enable the algorithm to not only adapt to diverse datasets but also to perform better when dealing with issues of class imbalance and data sparsity.

To strategically balance the influence of labeled and unlabeled data within our model, we introduce the supervision rate η. The larger the value of η, the greater the weight of the supervision term, and the greater the influence of prior knowledge from labeled data on the clustering results. This approach aims to optimize the model's performance by carefully calibrating the weight given to each data type. We further innovate with the adaptive parameter α, which, akin to η, fine-tunes the labeled data's overall impact on our algorithm. Unlike η, which requires empirical determination and manual adjustment, α dynamically adjusts based on the formula $\alpha = \frac{N}{L}$. Therefore, this adjustment is contingent upon the proportional dimensions of the labeled and unlabeled pattern collections, aligning the influence of labeled pixels with their proportion in the dataset to ensure they are adequately considered.

$$b_j = \begin{cases} 1 & \text{if pattern } \boldsymbol{x}_j \text{ is labeled} \\ 0 & \text{otherwise} \end{cases} \tag{6}$$

In defining the presence of labels within our dataset, we employ a binary vector $\boldsymbol{b} = \left[b_j\right]_{j=1,2,\cdots,n}$ where the value of b_j is obtained from formula (6). This methodological choice serves to clearly demarcate labeled from unlabeled patterns, facilitating more precise algorithmic adjustments. The degree of membership for labeled samples is encapsulated in a matrix $\boldsymbol{F} = \left[f_{ij}\right]_{i=1,2,\cdots,c,j=1,2,\cdots,n}$ designed to quantitatively represent the affiliation of each sample to the identified classes. This matrix is pivotal in refining our model's classification accuracy by providing a structured framework to assess the certainty of each label association.

An iterative algorithm to minimize (5) can be developed through the assessment of centroids and memberships that meet the zero-gradient criterion. By applying Lagrange multipliers to uphold the conditions set in $\sum_{i=1}^{c} u_{ij} = 1$, the Lagrangian function $L(\boldsymbol{u}, \boldsymbol{v}, \boldsymbol{\lambda})$ is obtained, as shown in equation (7).

$$\begin{aligned} L(\boldsymbol{u},\boldsymbol{v},\boldsymbol{\lambda}) = (1-\eta)\sum_{i=1}^{C}\sigma_i\sum_{j=1}^{N}u_{ij}^m d_{ij}^2 \\ + \eta\alpha\sum_{i=1}^{C}\sum_{j=1}^{N}b_j\left(\left|u_{ij}-f_{ij}\right|^m + u_{ij}^m\right)d_{ij}^2 \\ + \sum_{j=1}^{N}\lambda_j\left(1-\sum_{i=1}^{C}u_{ij}\right) \end{aligned} \tag{7}$$

$\boldsymbol{\lambda} = \left[\lambda_j\right]_{j=1,2,\cdots,n}$ is a Lagrange multiplier used to enforce the constraint that the sum of membership degrees for each data point across all clusters equals one. This constraint ensures that each data point is fully assigned to the clusters, thereby maintaining the integrity of the clustering process.

Computing the partial derivative of (7) concerning u_{ij}, we obtain

$$\begin{aligned} \frac{\partial L(\boldsymbol{u},\boldsymbol{v},\boldsymbol{\lambda})}{\partial u_{ij}} = m(1-\eta)\sigma_i d_{ij}^2 u_{ij}^{m-1} \\ + m\eta\alpha b_j d_{ij}^2\left(\left|u_{ij}-f_{ij}\right|^{m-1} + u_{ij}^{m-1}\right) - \lambda_j \end{aligned} \tag{8}$$

Setting the partial derivative to zero, with $m = 2$, we have an explicit formula

$$u_{ij} = \frac{2\eta\alpha b_j d_{ij}^2 f_{ij} + \lambda_j}{2\left[(1-\eta)\sigma_i + 2\eta\alpha b_j\right]d_{ij}^2} \tag{9}$$

To solve for λ_j, using the constraint equation $\sum_{i=1}^{c} u_{ij} = 1$, we get

$$\sum_{i=1}^{C}\frac{2\eta\alpha b_j d_{ij}^2 f_{ij} + \lambda_j}{2\left[(1-\eta)\sigma_i + 2\eta\alpha b_j\right]d_{ij}^2} = 1 \tag{10}$$

Expressing λ_j, we find

$$\lambda_j = 2\times\frac{1-\sum_{i=1}^{C}\frac{\eta\alpha b_j f_{ij}}{(1-\eta)\sigma_i+2\eta\alpha b_j}}{\sum_{i=1}^{C}\frac{1}{\left[(1-\eta)\sigma_i+2\eta\alpha b_j\right]d_{ij}^2}} \tag{11}$$

Combining equations (9) and (11), we derive the necessary conditions for u_{ij} at the local minimum of the objective function

$$u_{ij} = \frac{\eta\alpha b_j d_{ij}^2 f_{ij} + \frac{1-\sum_{i=1}^{C}\frac{\eta\alpha b_j f_{ij}}{(1-\eta)\sigma_i+2\eta\alpha b_j}}{\sum_{i=1}^{C}\frac{1}{\left[(1-\eta)\sigma_i+2\eta\alpha b_j\right]d_{ij}^2}}}{\left[(1-\eta)\sigma_i + 2\eta\alpha b_j\right]d_{ij}^2} \tag{12}$$

The presence of the parameter m in the supervision term simplifies the iterative formula for u_{ij} into a concise expression. Utilizing other exponential forms would result in a more complex equation. When $\eta = 0$ and $\boldsymbol{\sigma} = [1, 1, \ldots, 1]$, (12) corresponds to the formula for determining membership values in standard FCM; when $\boldsymbol{\sigma} = [1, 1, \ldots, 1]$, then (12) corresponds to the equation for computing membership values in MFM-SFCM [32]. Similar to the SFCM algorithm, for any value of m other than 2, the optimization conditions require additional computational work. This is because u_{ij} and the Lagrange multipliers are now connected in the form of polynomial equations, the solutions of which need to be computed numerically. When $m \neq 2$, an alternative approach is to reconstruct the equations incorporating m according to formula (12). This paper focuses solely on the case where $m = 2$.

For the iterative formula regarding cluster centers v_i, taking the partial derivative of the objective function (5) with respect to v_i, we obtain

$$\begin{aligned} \frac{\partial L(\boldsymbol{u},\boldsymbol{v},\boldsymbol{\lambda})}{\partial v_i} = 2(1-\eta)\sigma_i\sum_{j=1}^{N}u_{ij}^m\left(v_i - x_j\right) \\ + 2\eta\alpha\sum_{j=1}^{N}b_j\left(\left|u_{ij}-f_{ij}\right|^m + u_{ij}^m\right)\left(v_i - x_j\right) \end{aligned} \tag{13}$$

Setting the partial derivative to zero yields

$$v_i = \frac{(1-\eta)\sigma_i\Sigma_{j=1}^{N}u_{ij}^m x_j + \eta\alpha\Sigma_{j=1}^{N}b_j\left(\left|u_{ij}-f_{ij}\right|^m + u_{ij}^m\right)x_j}{(1-\eta)\sigma_i\Sigma_{j=1}^{N}u_{ij}^m + \eta\alpha\Sigma_{j=1}^{N}b_j\left(\left|u_{ij}-f_{ij}\right|^m + u_{ij}^m\right)} \tag{14}$$

The iteration of these necessary conditions forms an algorithm to minimize the ICBF-MFSFCM objective function. Steps include:

(1) Obtain an initial estimate for centroids v_i.
(2) Calculate the membership using (12).
(3) Calculate centroids using (14).
(4) Return to step 2 and continue the process until convergence is achieved.

To prove that the calculations in step 2 of the ICBF-MFSFCM algorithm will definitely reduce the value of the objective function labeled as (5), it is only necessary to prove that the Hessian matrix concerning $u_{1j}, \ldots, u_{Cj}$ for each pixel j is positive definite. This $\boldsymbol{C} \times \boldsymbol{C}$ matrix will be diagonal, with diagonal elements p_i satisfying

$$\begin{aligned} p_i = m(1-\eta)\sigma_i d_{ij}^2(m-1)u_{ij}^{m-2} \\ + m\eta\alpha b_j d_{ij}^2\left\{(m-1)\left[\operatorname{sign}\left(u_{ij}-f_{ij}\right)\cdot\left|u_{ij}-f_{ij}\right|^{m-2}\right]\right. \\ \left. + (m-1)u_{ij}^{m-2}\right\} \end{aligned} \tag{15}$$

By substituting (12) into u_{ij} and since $|x_j - v_i| > 0$, each p_i is strictly positive, thus the Hessian matrix is positive definite.

Similarly, to prove that the calculations in step 3 of the ICBF-MFSFCM algorithm will definitely reduce the value of the objective function labeled as (5), it is only necessary

to prove that the Hessian matrix concerning $v_1, \ldots, v_C$ is positive definite. This $\boldsymbol{C} \times \boldsymbol{C}$ matrix will assume a diagonal form, where the diagonal entries q_i satisfying

$$q_i = 2(1-\eta)\,\sigma_i \sum_{j=1}^{N} u_{ij}^m + 2\eta\alpha \sum_{j=1}^{N} b_j \left(|u_{ij} - f_{ij}|^m + u_{ij}^m \right) \tag{16}$$

By substituting (14) into u_{ij} and since $|x_j - v_i| > 0$, $|u_{ij} - f_{ij}| > 0$, each q_i is strictly positive, thus the Hessian matrix is positive definite. In summary, it can be guaranteed that the ICBF-MFSFCM algorithm's objective function will gradually diminish progressively with every cycle of the algorithm.

Correctly selecting the $\boldsymbol{\sigma}$ parameter is crucial for achieving peak or nearly peak performance. The suitable $\boldsymbol{\sigma}$ value varies according to the image subject to clustering. From (5) and (12), it is apparent that this value is contingent upon the image's luminosity and the changes in intensity levels in relation to the centroids of each category. The appropriate $\boldsymbol{\sigma}$ and η values will be investigated through experimental studies in the experimental section of this paper.

IV. RESULT AND DISCUSSION

To verify capability of ICBF-MFSFCM in managing clustering operations, we evaluated the ICBF-MFSFCM algorithm using authentic DWI images supplied by a hospital. First, we describe the experimental setup and dataset. Then, we explore the selection of different parameters. Finally, we compare the clustering performance of the ICBF-MFSFCM algorithm with that of five other algorithms.

A. EXPERIMENTAL ENVIRONMENT

Unless otherwise specified, all experiments were conducted on a PC equipped with an Intel Core i7- 12800HX CPU at 4.80GHz, and Python 3.7 was the programming environment used.

B. EVALUATION METRICS

In our experiments, five evaluation metrics were used to assess the performance of all algorithms: Intersection over Union (IoU), Dice Coefficient (DSC), Surface DSC (SDSC), Precision, and Recall [34], [35]. They are used to measure the overlap extent between the segmentation outcomes and the gold standard, thereby quantitatively evaluating the segmentation effect.

The definition of IoU:

$$\mathrm{IoU} = \frac{|A \cap B|}{|A \cup B|} \tag{17}$$

The definition of DSC is as follows:

$$DSC = \frac{2|A \cap B|}{|A| + |B|} \tag{18}$$

wherein, A and B denote the pixel sets of the segmentation result and the baseline truth labels, respectively, $|A|$ and $|B|$ denote the size of these sets.

The Surface Dice Similarity Coefficient (Surface-DSC) is an indicator for evaluating the quality of image segmentation, with a particular emphasis on the similarity between segmentation surfaces. It assesses the performance of image segmentation algorithms by quantifying the consistency between the segmented surface and the true surface. Surface-DSC is especially suitable for those application scenarios that require high precision of segmentation surfaces, such as medical image segmentation, where accurate surface details are crucial for subsequent analysis and applications. The calculation of Surface-DSC is based on the traditional DSC, which measures the similarity between two samples by comparing their overlap. Unlike DSC, Surface-DSC focuses more on the overlap and consistency of surfaces rather than just the overall volume or area overlap. The calculation formula for SDSC is as follows:

$$\mathrm{Surface-DSC} = \frac{2 \times |S_p \cap S_r|}{|S_p| + |S_r|} \tag{19}$$

wherein: S_p represents the set of points on the predicted segmentation surface, S_r represents the set of points on the real segmentation surface, $|S_p \cap S_r|$ denotes the number of points matching or overlapping between the predicted and real surfaces, and S_p and S_r are the total number of points on the predicted and real surfaces, respectively. In practical applications, the point sets of surfaces can be defined by extracting points on the segmentation boundaries or by using specific algorithms to approximate the surface. Calculating the intersection between S_p and S_r typically requires defining a distance threshold to determine whether points on the two surfaces are sufficiently close to be considered overlapping or matching. The choice of this threshold depends on the specific application and the resolution of the images. Surface-DSC provides a method to measure the performance of image segmentation algorithms in terms of surface precision.

One other core evaluation metric is F1-score. Our F1-score calculation method focuses solely on lesions rather than averaging across all categories. Here, TP (True Positives) refers to the number of samples correctly identified as lesions; FP (False Positives) refers to the number of samples incorrectly classified as lesions from other categories; FN (False Negatives) refers to the number of lesion samples incorrectly classified as other categories. This approach allows for a more accurate assessment of the model's performance on the target task, avoiding the interference of class imbalance, and concentrates on improving the segmentation accuracy of lesion areas. This aligns with clinical needs and can more effectively guide model optimization.

C. DATA SET

As shown in Table 2, the experimental dataset was provided by Changshu No.1 People's Hospital. Two experienced radiologists selected 200 representative DWI images of patients with brain stroke from clinical data and completed the annotation of gold standard segmentation for comparison of segmentation results. The number of classes for image

TABLE 2. Dataset details.

Dataset ID	Source	Description	Number of Images	Data Format	Data Collection Time
Dataset A	Changshu No.1 People's Hospital	Cerebral Infarction DWI	20	DCM	2022/08
Dataset B	Changshu No.1 People's Hospital	Cerebral Infarction DWI	80	DCM	2023/02
Dataset C	Changshu No.1 People's Hospital	Cerebral Infarction DWI	100	DCM	2023/08

clustering was set to three: brain stroke lesions, other brain tissues, and background. We assume that each class has only one cluster center. This assumption is reasonable for the task of lesion segmentation in diffusion-weighted imaging (DWI) data for stroke, as each target area (particularly lesions and background) typically exhibits relatively consistent characteristics. Moreover, by assuming each class has only one cluster center, we can significantly enhance the consistency of the segmentation results.

D. PARAMETERS OPTIMIZATION

In this part, we employ a genetic algorithm with an elitist preservation strategy to determine the optimal values of the parameters $\eta \in [0, 1)$ and $\boldsymbol{\sigma}$ (a three-dimensional vector with element values between 0 and 1) for the ICBF-MFSFCM algorithm. First, we encode these parameters as chromosomes, using a real number encoding method to preserve the continuity of the parameters. The initial population size of the genetic algorithm is set to 80. Through selection, crossover (crossover rate of 0.8), and mutation (mutation rate of 0.05) operations, we carry out 40 generations of iterations to search for the optimal combination of parameters, retaining elite individuals in each iteration.

Our defined fitness function is based on the predictive performance of the algorithm, specifically selecting the Intersection over Union (IoU) between the segmentation results on the dataset and the standard segmentation as the fitness. Through iterative optimization, the algorithm identifies an optimal set of parameters. As illustrated in Figure 3, owing to the implementation of an elitist preservation strategy, the fitness of each generation is incremental. Experimental results show that the optimized parameter η is 0.74, while the optimal values for the three-dimensional vector $\boldsymbol{\sigma}$ are [1, 0.07, 0.14]. The iterative valuation process for these two parameters is illustrated in Figure 4 and Figure 5.

E. PARAMETER σ

In this experiment, we investigated the impact of different $\boldsymbol{\sigma}$ values on the algorithm's segmentation effectiveness. The algorithm starts with a non-random initialization, using the average values of each category with label information as

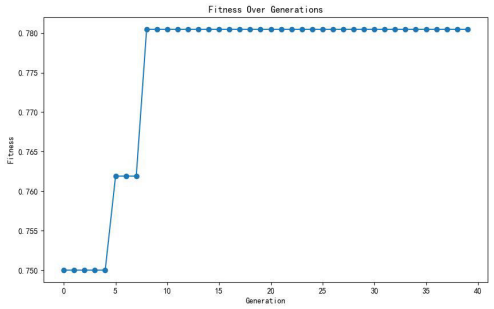

FIGURE 3. Fitness over generations.

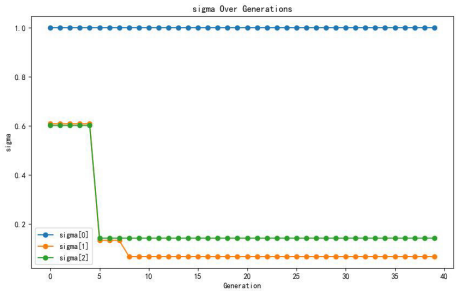

FIGURE 4. σ over generations.

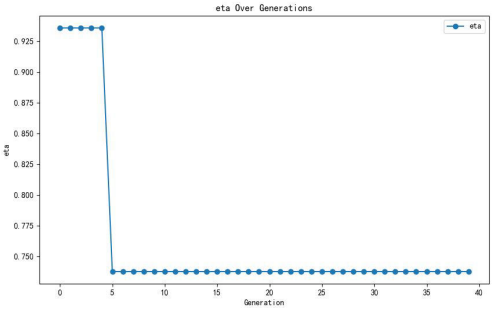

FIGURE 5. η over generations.

the initial clustering centers for the corresponding categories. Therefore, if there is no confusion of categories during the clustering process, σ_1 is the weight for the first category, i.e., brain stroke lesions, σ_2 for the second category, i.e., background, and σ_3 for the third category, i.e., other brain tissues. Let $m = 2$, $\eta = 0$, at this point, only the values of $\boldsymbol{\sigma}$ affect the segmentation effect of the algorithm. We employed a grid search method over $\left\{\boldsymbol{\sigma} \in \mathrm{R}^{1\times C} | \sigma_i \in [0, 1] \forall i\right\}$ to find the optimal values of the $\boldsymbol{\sigma}$ vector that yield the best segmentation effect on the dataset, aiming for the highest SDSC score during the optimization process.

The experimental results are shown in Figure 6. The first graph displays the relationship between the values of the vector $\boldsymbol{\sigma}$ and the SDSC score, and the second graph shows the relationship between the values of the vector $\boldsymbol{\sigma}$ and the IoU score, where the depth of color represents the size of the SDSC and IoU scores, with colors closer to yellow indicating higher scores. The horizontal axis is the multiple of

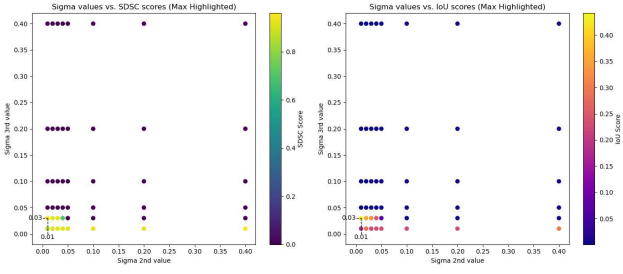

FIGURE 6. The impact of the σ value on the algorithm's segmentation effectiveness.

σ_2 relative to σ_1, and the vertical axis is the multiple of σ_3 relative to σ_1. Letting $\sigma_1 = 1$, we can clearly see several key points: (1) SDSC Score: The highest SDSC score appears when $\sigma_2 = 0.01$, $\sigma_3 = 0.03$, where the SDSC score is close to 0.96, indicating a very high structural similarity of the image. As σ_2, σ_3 increase, the SDSC score drops sharply to 0, showing a significant decrease in image similarity. (2) IoU Score: The highest IoU score is also observed at $\sigma_2 = 0.01, \sigma_3 = 0.03$, with a score of about 0.44, indicating that the accuracy of prediction peaks under this parameter setting. Similar to the SDSC score, the IoU score significantly decreases as σ_2, σ_3 increase. Therefore, it can be concluded that $\boldsymbol{\sigma} = (1, 0.01, 0.03)$ is an optimal value.

Figure 7 shows a DWI image from the dataset with a more severe class imbalance and correspondingly greater segmentation challenge. As an example, it can be observed that the entire contour of the lesion is correctly identified, so the SDSC score is high, reaching 0.96; however, a flaw is that a part of the area inside the lesion contour (the middle black part) was not correctly classified, so the corresponding IoU is 0.44. This demonstrates that with $\eta = 0$, i.e., without a supervisory component, our proposed algorithm with appropriate $\boldsymbol{\sigma}$ values can still successfully cluster the desired categories, thanks to the non-random initialization. If $\boldsymbol{\sigma} = (1, 1, 1)$ is set, the algorithm degenerates to the FCM algorithm, and the corresponding results will be shown in the algorithm comparison section below.

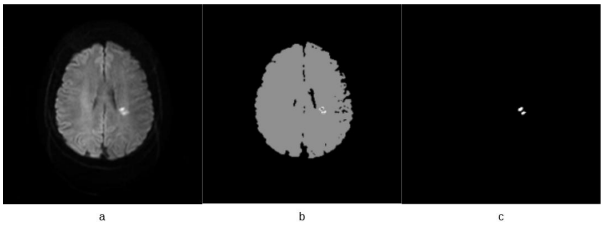

FIGURE 7. A DWI image with severe class imbalance in the dataset and its segmentation effect.

F. PARAMETER η

In this experiment, we investigate the impact of different η values on the algorithm's segmentation effectiveness and performance.

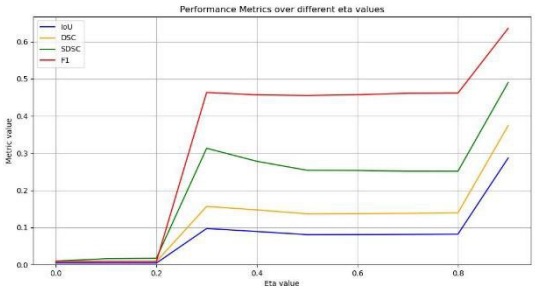

FIGURE 8. The average segmentation effect score for different values of η across 10 random sets of σ.

(1) We randomly generate 10 sets of $\boldsymbol{\sigma}$ vectors, each paired sequentially with η values of $[0.0, 0.1, \ldots, 0.9]$ for clustering segmentation on the dataset. We then calculate the average segmentation effectiveness scores for these different η values across the 10 sets of randomly generated $\boldsymbol{\sigma}$, thereby obtaining a general representation of the performance of different η values. From Figure 8, we can see that when $\eta = 0$, all evaluation metrics are almost zero. As the value of η increases, the segmentation performance of the algorithm generally improves.

(2) We select a set of $\boldsymbol{\sigma}$ values obtained previously in section 4.3.1, $\eta \in [0.0, 0.1, \ldots, 0.9]$, and experiment with its segmentation effectiveness on the dataset for other η in $\eta \in [0.0, 0.1, \ldots, 0.9]$ values. This set of values provides decent segmentation performance when $\eta = 0$. However, as shown in Figure 9, with the increase of η, the scores of all metrics decrease, but no metric drops to 0 even when $\eta = 0.9$.

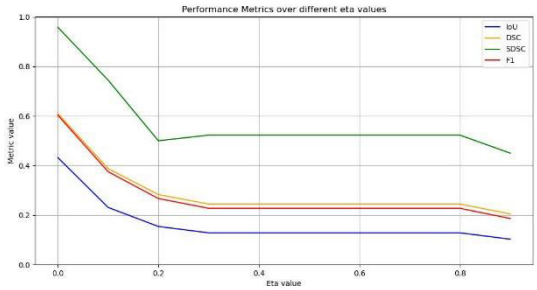

FIGURE 9. The segmentation effect of different values of η when $\sigma = (1, 0.01, 0.03)$.

(3) Setting $\eta = 0.5$, we employ a grid search algorithm to find a set of $\boldsymbol{\sigma}$ values that yield the best segmentation performance at $\eta = 0.5$, and similarly experiment with its segmentation effectiveness on the dataset for other $\eta \in [0.0, 0.1, \ldots, 0.9]$ values. Observing Figure 10, we find that at $\eta = 0.5$, scores for all metrics except recall reach their optimum. When $\eta \leq 0.4$, scores for multiple metrics drop to 0, resulting in complete segmentation failure, while for $\eta > 0.5$, scores for all metrics decline as η increases.

Synthesizing the above results, it is not difficult to observe that, for all average cases, a larger η value can endow the algorithm with better segmentation capability. However, once

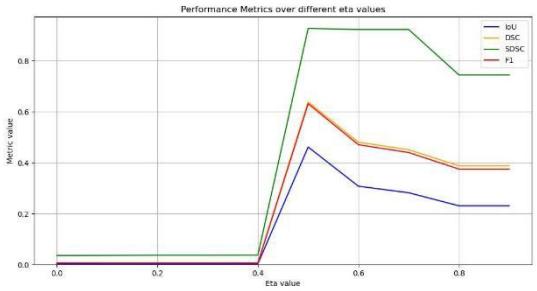

FIGURE 10. The segmentation effect with the optimal σ value at $\eta = 0.5$ across different values of η.

$\boldsymbol{\sigma}$ has been optimized, the value of η is no longer a case of "the larger, the better." On the contrary, the appropriate value of η at this point shows a strong correlation with $\boldsymbol{\sigma}$; even with $\eta = 0$, a suitably chosen $\boldsymbol{\sigma}$ can still successfully cluster the desired categories. Nevertheless, due to the larger η values emphasizing the guiding role of the supervisory term, the algorithm always maintains a decent segmentation performance, especially achieving commendable scores in SDSC. It's worth mentioning that the larger the η, the more it relies on the supervisory term, demanding higher accuracy of the provided supervisory data, which might lead to poorer generalization capability.

G. PERFORMANCE COMPARISON

In this section, we compared the segmentation performance of five algorithms on the dataset: Fuzzy C-Means clustering algorithm (FCM), Kernelized Generalized Fuzzy C-Means (KGFCM) [36], POCS-based clustering(POCS-based) [37], SFCM algorithm, and ICBF-MFSFCM algorithm. Among them, the KGFCM (Kernelized Generalized Fuzzy C-Means) algorithm is a fuzzy clustering algorithm based on kernel methods, which extends the traditional FCM algorithm. The KGFCM algorithm performs well in handling nonlinear data because it utilizes kernel tricks to map data into a high-dimensional feature space for clustering [36]. POCS (Projection Onto Convex Sets) is a commonly used method for optimization problems, and the POCS-based clustering algorithm is a technique that employs the POCS method for clustering. This method is primarily used to address the clustering of high-dimensional data, where the data is usually considered to exist within a low-dimensional subspace. The core idea of the POCS-based clustering algorithm is to cluster data points by iteratively projecting them onto different convex sets [37].

The FCM, SFCM, and ICBF-MFSFCM algorithms used the Euclidean distance in the experiments. Based on the composition of the dataset, the number of clusters was set to 3, representing brain stroke lesions, background, and other brain areas, respectively. Except for the ICBF-MFSFCM algorithm, which used the optimal parameters found through the genetic algorithm search mentioned in the parameter optimization section, the remaining algorithms used the optimal parameters identified via grid search strategies, as shown in Table 3.

TABLE 3. Table of parameters values used for testing algorithms.

Algorithm	Parameter
FCM	m∈(1,100]
KGFCM	P∈[3,10] m∈[2,10]
POCS-based	-
SFCM	$\alpha = 10^i, i \in$[-1,7] m=2

TABLE 4. Quantitative comparison of the effects of all algorithms on the DWI image dataset.

	FCM	KGFCM	POCS-based	SFCM	ICBF-MFSFCM
Dice	0.0784	0.0162	0.5416	0.7637	**0.8832**
IoU	0.0575	0.0077	0.4593	0.6655	**0.7911**
SDSC	0.0355	0.0011	0.4539	0.696	**0.9249**
F1	0.1142	0.0153	0.6444	0.7456	**0.8650**
Time	12.5491	164.2912	**4.0804**	7.9379	4.8073

Table 4 showcases the clustering outcomes of the 5 algorithms using the optimal parameters, measured by the average scores of the algorithms on the dataset images. The scores include: DSC, IoU, SDSC, F1-score, and the time taken for segmentation. Scores that are highest are emphasized in bold. We selected four DWI images from the dataset, where the area ratio of the lesion region progressively decreases, as examples to demonstrate the segmentation effectiveness of the five algorithms on images with varying areas in Figure 11.

Table 4 reveals that the ICBF-MFSFCM algorithm achieved the best average scores in DSC, IoU, SDSC, and F1-score. The reason for this can be found in Figure 11: With the four example DWI images, the area ratio of the lesion region decreases sequentially, the degree of class imbalance increases, and the difficulty of correct segmentation also increases. In the first example DWI image, where the lesion area is relatively large, all algorithms except KGFCM

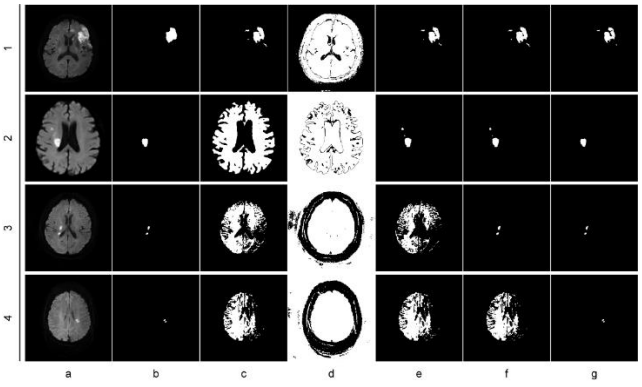

FIGURE 11. The segmentation effect on the example images. (a) Source image, (b) Gold standard segmentation, (c)FCM, (d) KGFCM, (e) POCS-based, (f) SFCM, (g) ICBF-MFSFCM.

essentially succeeded in segmentation; in the second example image, as the lesion area decreases, not only the KGFCM algorithm but also the FCM algorithm failed in segmentation; in the third example image, where the degree of class imbalance is severe, only the SFCM algorithm and the proposed ICBF-MFSFCM algorithm succeeded in segmentation; by the fourth example image, with the most severe class imbalance, the proposed ICBF-MFSFCM algorithm, thanks to the introduction of the class balance factor, became the sole success. Other algorithms, to varying extents, misclassified large areas as lesions. In summary, the proposed ICBF-MFSFCM algorithm achieved the best segmentation performance on the dataset.

V. CONCLUSION

This paper delves into the significance of high-quality medical image segmentation in the diagnosis and treatment of brain stroke and the challenges it faces. Through automated methods, such as decision tree classifiers, the certainty of lesion areas can be enhanced, promoting early detection and effective treatment. Nonetheless, image segmentation technology still encounters numerous challenges when processing DWI images and lesion segmentation, including image quality, algorithm complexity, and dependence on professional knowledge. To overcome these limitations, semi-supervised fuzzy clustering methods have been proposed and have shown significant potential, especially in handling complex images with noise and uncertainty. By introducing an interclass balance factor, the Interclass Balance Factor-based Membership Fusion Semi-supervised Fuzzy Clustering Algorithm (ICBF-MFSFCM) proposed in this study further improves the accuracy and efficiency of brain stroke DWI image segmentation, effectively addressing the issue of class imbalance. Through a series of experiments, the advantages of this algorithm in enhancing segmentation precision and robustness were verified, showcasing its potential application in the early diagnosis and treatment of brain stroke. The introduction of the interclass balance factor is not only an innovative attempt to address the issue of class imbalance in semi-supervised learning but also provides a new perspective to understand and handle the class dynamics within datasets. The practical application and validation of this approach will further demonstrate its value in enhancing model performance and fairness. The introduction of the interclass balance factor in the ICBF-MFSFCM algorithm addresses the common issue of class imbalance in medical datasets. This feature is particularly beneficial for medical conditions where the affected area is relatively small compared to the surrounding healthy tissue, such as in early-stage cancer detection or small lesion identification in liver disease.

However, the ICBF-MFSFCM algorithm still has some limitations. The introduction of hyperparameters η and $\boldsymbol{\sigma}$ makes the algorithm more flexible, providing it with the capability to adapt to different datasets and application scenarios. Nevertheless, this also brings the challenge of parameter selection. Although the grid search and genetic algorithm used in this paper can find relatively optimal parameter combinations to some extent, both methods increase the computational cost. This is especially true when dealing with large-scale datasets, where the parameter optimization process can become extremely time-consuming, thus limiting the efficiency and feasibility of the algorithm in practical applications. Future work will focus on finding ways to transform $\boldsymbol{\sigma}$ into an effective adaptive parameter.

REFERENCES

[1] D. V. Kumar and V. V. J. R. Krishniah, "An automated framework for stroke and hemorrhage detection using decision tree classifier," in *Proc. Int. Conf. Commun. Electron. Syst. (ICCES)*, Coimbatore, India, Oct. 2016, pp. 1–6, doi: 10.1109/CESYS.2016.7889861.

[2] A. Kumar, N. Upadhyay, P. Ghosal, T. Chowdhury, D. Das, A. Mukherjee, and D. Nandi, "CSNet: A new DeepNet framework for ischemic stroke lesion segmentation," *Comput. Methods Programs Biomed.*, vol. 193, Sep. 2020, Art. no. 105524, doi: 10.1016/j.cmpb.2020.105524.

[3] A. Subudhi, M. Dash, and S. Sabut, "Automated segmentation and classification of brain stroke using expectation-maximization and random forest classifier," *Biocybern. Biomed. Eng.*, vol. 40, no. 1, pp. 277–289, Jan. 2020, doi: 10.1016/j.bbe.2019.04.004.

[4] M. H. Hesamian, W. Jia, X. He, and P. Kennedy, "Deep learning techniques for medical image segmentation: Achievements and challenges," *J. Digit. Imag.*, vol. 32, no. 4, pp. 582–596, Aug. 2019, doi: 10.1007/s10278-019-00227-x.

[5] G. Litjens, T. Kooi, B. E. Bejnordi, A. A. A. Setio, F. Ciompi, M. Ghafoorian, J. A. W. M. van der Laak, B. van Ginneken, and C. I. Sánchez, "A survey on deep learning in medical image analysis," *Med. Image Anal.*, vol. 42, pp. 60–88, Dec. 2017, doi: 10.1016/j.media.2017.07.005.

[6] J. Peng and Y. Wang, "Medical image segmentation with limited supervision: A review of deep network models," *IEEE Access*, vol. 9, pp. 36827–36851, 2021, doi: 10.1109/ACCESS.2021.3062380.

[7] S. Minaee, Y. Boykov, F. Porikli, A. Plaza, N. Kehtarnavaz, and D. Terzopoulos, "Image segmentation using deep learning: A survey," *IEEE Trans. Pattern Anal. Mach. Intell.*, vol. 44, no. 7, pp. 3523–3542, Jul. 2022, doi: 10.1109/TPAMI.2021.3059968.

[8] I. R. I. Haque and J. Neubert, "Deep learning approaches to biomedical image segmentation," *Informat. Med. Unlocked*, vol. 18, Jan. 2020, Art. no. 100297, doi: 10.1016/j.imu.2020.100297.

[9] T. C. Kwee, T. Takahara, R. Ochiai, R. A. J. Nievelstein, and P. R. Luijten, "Diffusion-weighted whole-body imaging with background body signal suppression (DWIBS): Features and potential applications in oncology," *Eur. Radiol.*, vol. 18, no. 9, pp. 1937–1952, Sep. 2008, doi: 10.1007/s00330-008-0968-z.

[10] F. Shi, J. Cheng, L. Wang, P. Yap, and D. Shen, "Super-resolution reconstruction of diffusion-weighted images using 4D low-rank and total variation," in *Proc. MICCAI Workshop*, Munich, Germany, Oct. 2015, pp. 15–25, doi: 10.1007/978-3-319-28588-7_2.

[11] J. J. Mathew, A. James, C. Kesavadas, and J. S. Paul, "Diffusion sensitivity enhancement filter for raw DWIs," *IET Comput. Vis.*, vol. 12, no. 7, pp. 950–956, Oct. 2018, doi: 10.1049/iet-cvi.2018.5213.

[12] Y. Guo, Z. Cui, Z. Yang, X. Wu, and S. Madani, "Non-local DWI image super-resolution with joint information based on GPU implementation," *Comput., Mater. Continua*, vol. 61, no. 3, pp. 1205–1215, 2019, doi: 10.32604/cmc.2019.06029.

[13] B. Fan, Z. Li, and J. Gao, "DwiMark: A multiscale robust deep watermarking framework for diffusion-weighted imaging images," *Multimedia Syst.*, vol. 28, no. 1, pp. 295–310, Feb. 2022, doi: 10.1007/s00530-021-00835-0.

[14] L. Santos, R. Veras, K. Aires, L. Britto, and V. Machado, "Medical image segmentation using seeded fuzzy C-means: A semi-supervised clustering algorithm," in *Proc. Int. Joint Conf. Neural Netw. (IJCNN)*, Jul. 2018, pp. 1–7, doi: 10.1109/IJCNN.2018.8489401.

[15] J. Miao, X. Zhou, and T.-Z. Huang, "Local segmentation of images using an improved fuzzy C-means clustering algorithm based on self-adaptive dictionary learning," *Appl. Soft Comput.*, vol. 91, Jun. 2020, Art. no. 106200, doi: 10.1016/j.asoc.2020.106200.

[16] J. Chen, Y. Li, L. P. Luna, H. W. Chung, S. P. Rowe, Y. Du, L. B. Solnes, and E. C. Frey, "Learning fuzzy clustering for SPECT/CT segmentation via convolutional neural networks," *Med. Phys.*, vol. 48, no. 7, pp. 3860–3877, Jul. 2021, doi: 10.1002/mp.14903.
[17] Y. K. Dubey, M. M. Mushrif, and K. Mitra, "Segmentation of brain MR images using rough set based intuitionistic fuzzy clustering," *Biocybern. Biomed. Eng.*, vol. 36, no. 2, pp. 413–426, 2016, doi: 10.1016/j.bbe.2016.01.001.
[18] T. M. Tuan, L. H. Son, and L. B. Dung, "Dynamic semi-supervised fuzzy clustering for dental X-ray image segmentation: An analysis on the additional function," *J. Comput. Sci. Cybern.*, vol. 31, no. 4, p. 323, Jan. 2016, doi: 10.15625/1813-9663/31/4/7234.
[19] L. H. Son and T. M. Tuan, "A cooperative semi-supervised fuzzy clustering framework for dental X-ray image segmentation," *Expert Syst. Appl.*, vol. 46, pp. 380–393, Mar. 2016, doi: 10.1016/j.eswa.2015.11.001.
[20] A. Kumar, H. S. Bhadauria, and A. Singh, "Semi-supervised Otsu based hyperbolic tangent Gaussian kernel fuzzy C-mean clustering for dental radiographs segmentation," *Multimedia Tools Appl.*, vol. 79, nos. 3–4, pp. 2745–2768, Jan. 2020, doi: 10.1007/s11042-019-08268-8.
[21] M. A. Balafar, "Fuzzy C-mean based brain MRI segmentation algorithms," *Artif. Intell. Rev.*, vol. 41, no. 3, pp. 441–449, Mar. 2014, doi: 10.1007/s10462-012-9318-2.
[22] H. Liu and S.-T. Huang, "Evolutionary semi-supervised fuzzy clustering," *Pattern Recognit. Lett.*, vol. 24, no. 16, pp. 3105–3113, Dec. 2003, doi: 10.1016/s0167-8655(03)00177-6.
[23] A. Bouchachia and W. Pedrycz, "Enhancement of fuzzy clustering by mechanisms of partial supervision," *Fuzzy Sets Syst.*, vol. 157, no. 13, pp. 1733–1759, Jul. 2006, doi: 10.1016/j.fss.2006.02.015.
[24] P. A. Lopes and H. A. Camargo, "Semi-supervised clustering in fuzzy rule generation," in *Proc. 8th Encontro Nacional Inteligência Artif. (ENIA)*, Natal, Brazil, Jul. 2011, pp. 228–239.
[25] N. V. Chawla, K. W. Bowyer, L. O. Hall, and W. P. Kegelmeyer, "SMOTE: Synthetic minority over-sampling technique," *J. Artif. Intell. Res.*, vol. 16, pp. 321–357, Jun. 2002, doi: 10.1613/jair.953.
[26] Z. Huang, "Extensions to the k-means algorithm for clustering large data sets with categorical values," *Data Mining Knowl. Discovery*, vol. 2, no. 3, pp. 283–304, 1998, doi: 10.1023/a:1009769707641.
[27] A. Strehl and J. Ghosh, "Cluster ensembles—A knowledge reuse framework for combining multiple partitions," *J. Mach. Learn. Res.*, vol. 3, pp. 583–617, Mar. 2003, doi: 10.1162/153244303321897735.
[28] M. Ester, H.-P. Kriegel, J. Sander, and X. Xu, "A density-based algorithm for discovering clusters in large spatial databases with noise," in *Proc. 2nd Int. Conf. Knowl. Discovery Data Mining*. Portland, OR, USA: AAAI Press, Aug. 1996, pp. 226–231.
[29] M. Ankerst, M. M. Breunig, H.-P. Kriegel, and J. Sander, "OPTICS: Ordering points to identify the clustering structure," *ACM SIGMOD Rec.*, vol. 28, no. 2, pp. 49–60, Jun. 1999, doi: 10.1145/304181.304187.
[30] W. Pedrycz and J. Waletzky, "Fuzzy clustering with partial supervision," *IEEE Trans. Syst., Man, Cybern. B, Cybern.*, vol. 27, no. 5, pp. 787–795, Oct. 1997, doi: 10.1109/3477.623232.
[31] K. Wagstaff, C. Cardie, S. Rogers, and S. Schrödl, "Constrained K-means clustering with background knowledge," in *Proc. 18th Int. Conf. Mach. Learn.* San Francisco, CA, USA: Morgan Kaufmann, 2001, pp. 577–584.
[32] B. Zhang, L. Huang, J. Wang, L. Zhang, Y. Wu, Y. Jiang, and K. Xia, "Semi-supervised fuzzy C means based on membership integration mechanism and its application in brain infarction lesion segmentation in DWI images," *J. Intell. Fuzzy Syst.*, vol. 46, no. 1, pp. 2713–2726, Jan. 2024, doi: 10.3233/jifs-234148.
[33] J. C. Bezdek, R. Ehrlich, and W. Full, "FCM: The fuzzy c-means clustering algorithm," *Comput. Geosci.*, vol. 10, nos. 2–3, pp. 191–203, Jan. 1984, doi: 10.1016/0098-3004(84)90020-7.
[34] H.-H. Chang, A. H. Zhuang, D. J. Valentino, and W.-C. Chu, "Performance measure characterization for evaluating NeuroImage segmentation algorithms," *NeuroImage*, vol. 47, no. 1, pp. 122–135, Aug. 2009, doi: 10.1016/j.neuroimage.2009.03.068.
[35] H. Rezatofighi, N. Tsoi, J. Gwak, A. Sadeghian, I. Reid, and S. Savarese, "Generalized intersection over union: A metric and a loss for bounding box regression," 2019, *arXiv:1902.09630*.
[36] A. Gupta and S. Das, "On the unification of k-harmonic means and fuzzy c-Means clustering problems under kernelization," in *Proc. 9th Int. Conf. Adv. Pattern Recognit. (ICAPR)*, Bengaluru, India, Dec. 2017, pp. 1–6, doi: 10.1109/ICAPR.2017.8593078.
[37] L.-A. Tran, H. M. Deberneh, T.-D. Do, T.-D. Nguyen, M.-H. Le, and D.-C. Park, "POCS-based clustering algorithm," in *Proc. Int. Workshop Intell. Syst. (IWIS)*, Ulsan, South Korea, Aug. 2022, pp. 1–6, doi: 10.1109/IWIS56333.2022.9920762.

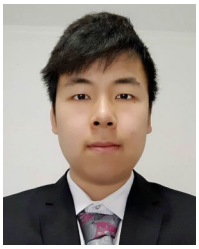

BENFEI ZHANG is currently pursuing the master's degree with the School of Artificial Intelligence and Computer Science, Jiangnan University, Wuxi, China. His research interests include MRI reconstruction, medical image segmentation, and machine learning.

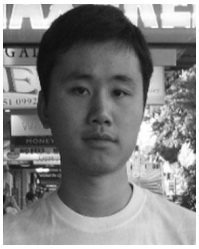

YIZHANG JIANG (Senior Member, IEEE) received the Ph.D. degree from Jiangnan University, Wuxi, China, in 2015.

He has been a Research Assistant with the Department of Computing, The Hong Kong Polytechnic University, Hong Kong, for two years. He is the author/co-author of more than 60 research articles in international/national journals, including IEEE TRANSACTIONS ON FUZZY SYSTEMS, IEEE TRANSACTIONS ON NEURAL NETWORKS AND LEARNING SYSTEMS, IEEE TRANSACTIONS ON CYBERNETICS, and *Information Sciences*. His research interests include pattern recognition, intelligent computation, and their applications. He has been an Associate Editor of IEEE ACCESS, since 2019. He has also served as a Lead Guest Editor or a Guest Editor for several international journals, such as IEEE/ACM TRANSACTIONS ON COMPUTATIONAL BIOLOGY AND BIOINFORMATICS and IEEE TRANSACTIONS ON COMPUTATIONAL SOCIAL SYSTEMS.

KAIJIAN XIA received the B.S. degree from the School of Computer Science and Engineering from Soochow University, Suzhou, Jiangsu, China, the M.S. degree from the School of Information and Engineering, Jiangnan University, Wuxi, Jiangsu, and the Ph.D. degree from the School of Information and Control Engineering, China University of Mining and Technology, Xuzhou, Jiangsu. He is currently a Senior Engineer of computer science with Changshu Hospital Affiliated to Soochow University, Changshu, Jiangsu; a Professor of medical information with the University of Malaya, Malaya; and a Graduate Supervisor with Jiangnan University. He is the author/co-author of more than 90 research papers in international/national journals, including IEEE TRANSACTIONS ON INDUSTRIAL INFORMATICS, IEEE TRANSACTIONS ON INTELLIGENT TRANSPORTATION SYSTEM, IEEE/ACM TRANSACTIONS ON COMPUTATIONAL BIOLOGY AND BIOINFORMATICS, *ACM Transactions on Internet Technology*, *ACM Transactions Multimedia Computing, Communications, and Applications*, and *Information Sciences*. His research interests include intelligent medical information, image processing, and machine learning.